MASTER

UCID- 17973

Lawrence Livermore Laboratory

EFFECT OF PORE SIZE DISTRIBUTION AND FLOW SEGREGATION ON DISPERSION IN POROUS MEDIA

R. G. Carbonell

November, 1978

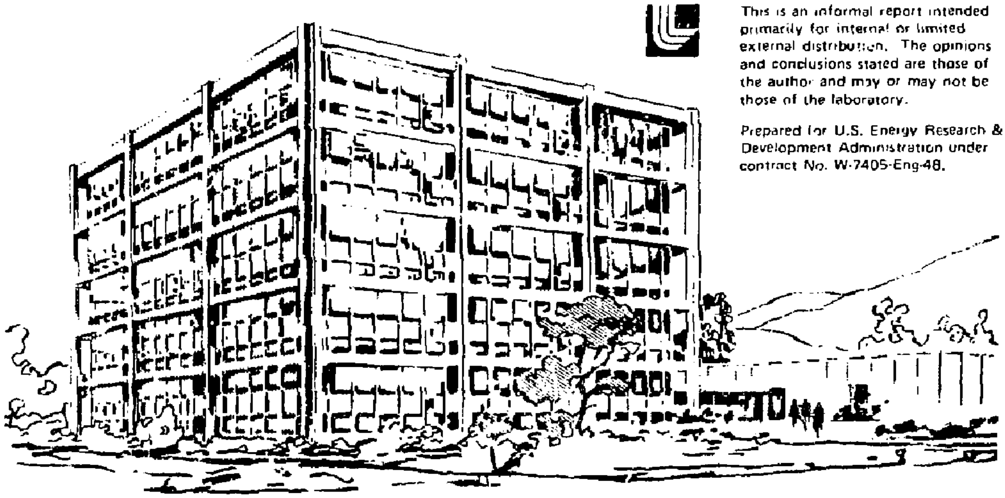

This is an informal report intended primarily for internal or limited external distribution. The opinions and conclusions stated are those of the author and may or may not be those of the laboratory.

Prepared for U.S. Energy Research & Development Administration under contract No. W-7405-Eng-48.

EFFECT OF PORE SIZE DISTRIBUTION AND FLOW SEGREGATION ON DISPERSION IN POROUS MEDIA

R. G. Carbonell

Department of Chemical Engineering
University of California
Davis, California 95616

Abstract

In order to study the effect of the pore size distribution and flow segregation on dispersion in a porous media, we consider the dispersion of solute in an array of parallel pores. Equations are obtained for the dispersion coefficient in laminar and turbulent flow, as a function of the particle Peclet number. The theory fits quite well cumulative experimental data from various researchers in the Peclet number range from 10^{-3} to 10^{6}. The model also predicts some trends, backed by experimental data, regarding the effect of particle size, particle size distribution and fluid velocity on dispersion.

1. Introduction

The effect of the distribution of pore sizes on the magnitude of the dispersion coefficient in a porous media, is a complex problem due to the complicated geometry and flow distribution around individual particles. One approach to this problem was presented by Greenkorn and Kessler [1] and Haring and Greenkorn [2]. They extended the straight pore model of Saffman [3] and De Josselin De Jong [4] to include a distribution of pore radii and pore lengths. This approach is statistical in nature, since it is based on a random walk of a marked particle of fluid whose probability of passing through a given pore is directly proportional to the volumetric flow rate in the pore. This type of model is useful since it can provide an idea of how sensitive the dispersion coefficient is to the distribution of pore sizes, and can generate both longitudinal and transverse dispersion coefficients. Indeed, Greenkorn and Kessler [1] cite results indicating that the ratio of longitudinal to transverse dispersion coefficients is quite sensitive to changes in the pore size distribution. One disadvantage of this approach, is that it neglects the details of how the hydrodynamics of the flow in the pores would affect dispersion. In particular, it is not possible to consider laminar versus turbulent flow differences, or how the fluid properties, the Reynolds and Schmidt numbers, would affect dispersion. To this end, we consider the simplest type of model for a porous media that would allow one to include flow profiles and known values of dispersion coefficients in individual pores, and that one can solve exactly. By studying dispersion in an array of parallel pores, one can vary the flow from laminar to turbulent, change the shape of the pore, and vary the pore size distribution. Interestingly enough, the results of this model give very close agreement witn the Peclet number dependence of measured dispersion coefficients

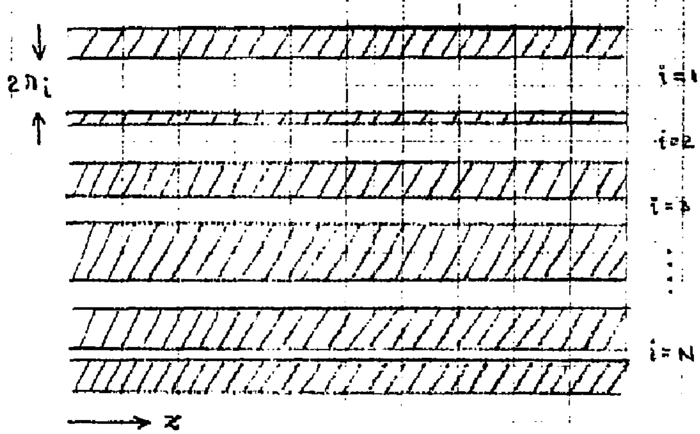

Figure 1

Parallel pore model. — OMIT

in packed beds. In addition, it predicts trends on how the dispersion coefficient varies with the spread and the mean value of the particle size distribution that have been verified experimentally. The general problem of dispersion caused by segregated channels in a porous media is also of interest in the tracer study of fields to be used for coal gasification.

2. The Dispersion Coefficient

Consider an array of N straight parallel pores as shown in Figure 1. Each pore has a radius r_i and an area-averaged fluid velocity in the z direction $\langle v_z \rangle_i$. We assume that in each pore the flow is fully developed, and that we can describe the area-averaged concentration $\langle c \rangle_i$ of an inert solute in the pore in terms of a dispersion equation,

$$\frac{\partial \langle c \rangle_i}{\partial t} + \langle v_z \rangle_i \frac{\partial \langle c \rangle_i}{\partial z} = D_i \frac{\partial \langle c \rangle_i}{\partial z} \qquad (1)$$

where D_i is the dispersion coefficient in pore i. Now we define an area-averaged concentration for the porous media, at a given z, in terms of the area-averaged concentrations in each pore, namely

$$\{c\} = A_p^{-1} \sum_{i=1}^{N} \langle c \rangle_i \, A_i \qquad (2)$$

where A_i is the area of each pore and A_p is the total pore area,

$$A_p = \sum_{i=1}^{N} A_i \qquad (3)$$

Note that in Eq. (2) all the $\langle c \rangle_i$ are properly weighted by their corresponding fluid area so that $\{c\}$ corresponds to the intrinsic phase-averaged concentration of solute in the porous media [5]. If we multiply Eq. (1) by A_i, sum over all i from 1 to N and divide by A_p, after some manipulations, one obtains,

$$\frac{\partial\{c\}}{\partial t} + \{v_z\}\frac{\partial\{c\}_b}{\partial z} = \{D\}\frac{\partial^2\{c\}_D}{\partial z^2} \tag{4}$$

where $\{v_z\}$ is the area-averaged fluid velocity in the porous media,

$$\{v_z\} = A_p^{-1}\sum_{i=1}^{N} \langle v_z\rangle_i A_i, \tag{5}$$

$\{D\}$ is an area-averaged dispersion coefficient,

$$\{D\} = A_p^{-1}\sum_{i=1}^{N} D_i A_i \tag{6}$$

$\{c\}_b$ is a bulk-averaged concentration,

$$\{c\}_b = \frac{\sum_{i=1}^{N} \langle c\rangle_i \langle v_z\rangle_i A_i}{\{v_z\} A_p} \tag{7}$$

and $\{c\}_D$ is a concentration weighted by the dispersion coefficient in each pore,

$$\{c\}_D = \frac{\sum_{i=1}^{N} \langle c\rangle_i D_i A_i}{\{D\} A_p} \tag{8}$$

Equation (4) is not much use in its current form since it contains three different dependent variables and the parameters depend on individual pore concentrations. What we would like to have is a dispersion equation that would give us a reasonable approximation for $\{c\}$. Consider a dispersion equation for the porous media of the form,

$$\frac{\partial\{c\}^*}{\partial t} + \{v_z\}\frac{\partial\{c\}^*}{\partial z} = \{D\}^*\frac{\partial^2\{c\}^*}{\partial z^2} \tag{9}$$

whose solution $\{c\}^*$ will not equal to $\{c\}$ point by point, but which will have the same zeroth, first and second moments in the axial direction,

$$m_k = \int_{-\infty}^{\infty} z^k\{c\}^* dz = \int_{-\infty}^{\infty} z^k\{c\}dz, \quad k = 0, 1, 2 \tag{10}$$

If we assume that for a pulsed system,

$$\{c\} = \frac{\partial\{c\}}{\partial z} = 0 \quad \text{at} \quad z = \pm\infty, \tag{11}$$

take the zeroth and first moments of Eqs. (4) and (9) and use property (10) we find that,

$$\frac{\partial m_o}{\partial t} = 0, \tag{12}$$

and

$$m_{ob} = m_o \tag{13}$$

This last criterion will be satisfied whenever a dispersion model is applicable (see appendix). Taking the second moment of Eqs. (4) and (9) and equating the results, we obtain an equation for the dispersion coefficient,

$$\{D\}^* = \{D\}\frac{m_{oD}}{m_o} + \{v_z\}\left(\frac{m_{1b} - m_1}{m_o}\right) \tag{14}$$

where,

$$m_{oD} = \int_{-\infty}^{\infty} \{c\}_D dz, \qquad (15)$$

and

$$m_{1b} = \int_{-\infty}^{\infty} z\{c\}_b dz \qquad (16)$$

The first term in Eq. (14) may be simplified if we take the zeroth moment of Eqs. (2) and (8),

$$m_{oD} = \frac{1}{\{D\}A_p} \sum_{i=1}^{N} D_i A_i m_{oi}, \qquad (17)$$

$$m_o = \frac{1}{A_p} \sum_{i=1}^{N} A_i m_{oi} \qquad (18)$$

where

$$m_{oi} = \int_{-\infty}^{\infty} \langle c \rangle_i dz \qquad (19)$$

is the zeroth moment of the concentration in pore i. Dividing Eq. (17) by Eq. (18) and multiplying by $\{D\}$ we find,

$$\{D\} \frac{m_{oD}}{m_o} = \frac{\sum_{i=1}^{N} D_i A_i m_{oi}}{\sum_{i=1}^{N} A_i m_{oi}} \qquad (20)$$

The quantity $A_i m_{oi}$ is the total amount of solute in pore i,

$$M_i = A_i m_{oi} \qquad (21)$$

while the total amount of solute in the porous media is,

$$M = \sum_{i=1}^{N} A_i m_{oi} \tag{22}$$

Defining the fraction of the total amount of solute that is present in pore i,

$$\omega_i = M_i/M, \tag{23}$$

$$\sum_{i=1}^{N} \omega_i = 1, \tag{24}$$

we can write Eq. (20) simply as,

$$\{D\} \frac{m_{oD}}{m_o} = \sum_{i=1}^{N} D_i \omega_i \tag{25}$$

Since the pores are not interconnected, ω_i is a constant for each i whose value depends on how the solute was originally distributed into the pores. The most reasonable way of doing this is to distribute the solute according to the ratio of the volumetric flow rate in each pore to the total volumetric flow rate,

$$\omega_i = \frac{\langle v_z \rangle_i A_i}{\{v_z\} A_p} \tag{26}$$

The second term in Eq. (14) may be similarly simplified. Taking the first moment of Eq. (7) and (2) and using Eq. (18), one can show that,

$$\frac{m_{1b} - m_1}{m_o} = M^{-1} \sum_{i=1}^{N} m_{1i} A_i \left[\frac{\langle v_z \rangle_i}{\{v_z\}} - 1 \right] \tag{27}$$

where m_{1i} is the first moment of the concentration in pore i,

$$m_{1i} = \int_{-\infty}^{\infty} z\langle c \rangle_i \, dz \tag{28}$$

We can obtain an expression for m_{1i} in terms of m_{oi} if we take the first moment of Eq. (1) and integrate the result,

$$m_{1i} = m_{oi}\langle v \rangle_i t \tag{29}$$

where we have used the initial condition that the average position of the pulse at $t = 0$ is zero. Using Eq. (29), (27) and (23), the second term in Eq. (14) becomes,

$$\{v_z\} \left[\frac{m_{1b} - m_1}{m_o} \right] = \{v_z\} \; t \sum_{i=1}^{N} \langle v_z \rangle_i \; \omega_i \left[\frac{\langle v_z \rangle}{\{v_z\}} - 1 \right] \tag{30}$$

Using Eq. (30) and (25), we find the final expression for the dispersion coefficient, Eq. (14),

$$\{D\}^* = \sum_{i=1}^{N} D_i \omega_i + \{v_z\}t \sum_{i=1}^{N} \langle v_z \rangle_i \; \omega_i \left[\frac{\langle v_z \rangle_i}{\{v_z\}} - 1 \right] \tag{31}$$

Several aspects of Eq. (31) are worth mentioning. The quantity $\{D\}^*$ is now expressed simply as a function of the flow hydrodynamics of each individual pore through the terms $\langle v_z \rangle_i$ and D_i. The first term is the contribution to dispersion from the shape of the velocity profile in each pore.

The second term is the contribution to dispersion from the differences in the fluid velocities in each pore. These differences cause the solute to "spread" due primarily to a convective effect. Note that it does not depend on D_i. Since the pores are not connected, naturally this term is time-dependent and would become very important for large times. The effect of the distribution of pore sizes is taken into account by the fact that both D_i and $\langle v_z \rangle_i$ are functions of r_i. We now study this effect by introducing the appropriate expressions for $\langle v_z \rangle_i$ and D_i for the case of laminar and turbulent flow.

3. Laminar Flow Case

In laminar flow, the area-averaged velocity in cylindrical pores is governed by the Hagen-Poiseuille equation [6],

$$\langle v_z \rangle_i = \frac{r_i^2}{8\mu} \left(\frac{\Delta p}{L}\right) \tag{32}$$

while the dispersion coefficient was derived by Taylor [7] and later modified to include molecular diffusion in the axial direction by Aris [8],

$$D_i = \mathcal{D} + \frac{\langle v_z \rangle_i \, r_i^2}{48\, \mathcal{D}} \tag{33}$$

where $\mathcal{D}$ is the molecular diffusivity. Using Eqs. (32) and (5) we can express $\langle v_z \rangle_i$ in terms of $\{v_z\}$,

$$\langle v_z \rangle_i = \{v_z\} \frac{r_i^2 \sum_{i=1}^{N} r_i^2}{\sum_{i=1}^{N} r_i^4} \tag{34}$$

while substituting (34) into (33) we can write D_i in terms of $\{v_z\}$,

$$D_i = \mathcal{D} + \frac{\{v_z\}^2 \, r_i^6}{48\mathcal{D}} \left(\frac{\sum_{i=1}^{N} r_i^2}{\sum_{i=1}^{N} r_i^4} \right) \tag{35}$$

Similarly, Eq. (26) for ω_i becomes,

$$\omega_i = \frac{r_i^4}{\sum_{i=1}^{N} r_i^4} \tag{36}$$

Substituting Eqs. (34), (35) and (36) into Eq. (31) for $\{D\}^*$ leads to,

$$\{D\}^* = \mathcal{D} + \frac{\{v_z\}^2}{48\mathcal{D}} \, \frac{\sum_{i=1}^{N} r_i^{10} \left(\sum_{i=1}^{N} r_i^2 \right)^2}{\left(\sum_{i=1}^{N} r_i^4 \right)^3} + \{v_z\}^2 t \, \frac{\sum_{i=1}^{N} r_i^2}{\left(\sum_{i=1}^{N} r_i^4 \right)^2} \left[\frac{\left(\sum_{i=1}^{N} r_i^2 \right) \left(\sum_{i=1}^{N} r_i^8 \right)}{\sum_{i=1}^{N} r_i^4} - \sum_{i=1}^{N} r_i^6 \right] \tag{37}$$

If we represent the nth moment of the pore size distribution by the summations,

$$\overline{r^n} = \frac{1}{N} \sum_{i=1}^{N} r_i^n , \quad n = 1, 2, 3.... \tag{38}$$

Eq. (38) reduces to,

$$\{D\}^* = D + \frac{\{v_z\}^2}{48D} \frac{\overline{r^{10}}(\overline{r^2})^2}{(\overline{r^4})^3} + \{v_z\}^2 t \frac{\overline{r^2}}{(\overline{r^4})^2}\left[\frac{\overline{r^2}\,\overline{r^8}}{\overline{r^4}} - \overline{r^6}\right] . \tag{39}$$

The second term on the right hand side is a Taylor dispersion term for the laminar velocity profile properly modified to take into account the pore size distribution. The second term is the spread due to velocity differences between the pores. Note that $\{D\}^*$ depends on the higher moments of the pore size distribution, indicating a strong dependence on the spread of the distribution.

In order to investigate this effect, we considered the possibility that the pore size distribution could be described by a Gaussian distribution with standard deviation σ and average pore radius $\bar{r}$. Fortunately, there are generating function techniques that allow one to calculate all the moments of the Gaussian distribution [9]. Substituting these into Eq. (39) we obtain,

$$\{D_T\}^* = D + \frac{\{v_z\}^2 \bar{r}^2}{48D} f_1(\xi) + \{v_z\}^2 t \, f_2(\xi) \tag{40}$$

where $\xi = \sigma/\bar{r}$ and the functions f_1 and f_2 are given in the appendix and plotted in Figure 2. As $\xi \to 0$, all the pores are the same size, the function $f_1 \to 1.0$ while $f_2 \to 0$, and one recovers the Taylor-Aris result from Eq. (40) with the radius equal to $\bar{r}$. As the pore size distribution becomes broader, ξ increases, and both f_1 and f_2 increase considerably, indicating a strong dependence of the dispersion coefficient on the spread of the pore size distribution.

One can follow the same procedure to find an equation analogous to (39) for the case of rectangular pores of width $2\ell_1$, and infinitely wide in the direction perpendicular to flow,

$$\{D\}^* = \mathcal{D} + \frac{2}{105\mathcal{D}}\{v_z\}^2 \frac{\overline{\ell^9}\,(\overline{\ell})^2}{(\overline{\ell^3})^2} + \{v_z\}^2 t \frac{\overline{\ell}}{(\overline{\ell^3})^2}\left[\frac{\overline{\ell^7}\,\overline{\ell}}{\overline{\ell^3}} - \overline{\ell^5}\right] \tag{41}$$

where the $\overline{\ell^n}$ represent the nth moment of the distribution of pore sizes. The quantity 2/105 replaces the 1/48 for the cylindrical pore case and the moment dependence is different. Using the results for the moments of a Gaussian distribution in the appendix, Eq. (42) can be written in a form analogous to Eq. (40),

$$\{D\}^* = \mathcal{D} + \frac{2}{105}\frac{\{v_z\}^2\,\overline{\ell}^2}{\mathcal{D}} f_1(\xi) + \{v_z\}^2 t\, f_2(\xi) \tag{42}$$

with $f_1(\xi)$ and $f_2(\xi)$ for rectangular gaps plotted in Figure 2. The great similarity between f_1 and f_2 for rectangular and cylindrical gaps indicates that there will not be much difference in the dispersion coefficients calculated from Eqs. (40) and (42). For practical purposes one would expect ξ to be less than or equal to 1 for most distributions.

We can put Eq. (9), and Eq. (40) in dimensionless form,

$$\frac{\partial\{C\}^*}{\partial\theta} + \frac{\partial\{C\}^*}{\partial Z} = D^* \frac{\partial^2\{C\}^*}{\partial Z^2}\ , \tag{43}$$

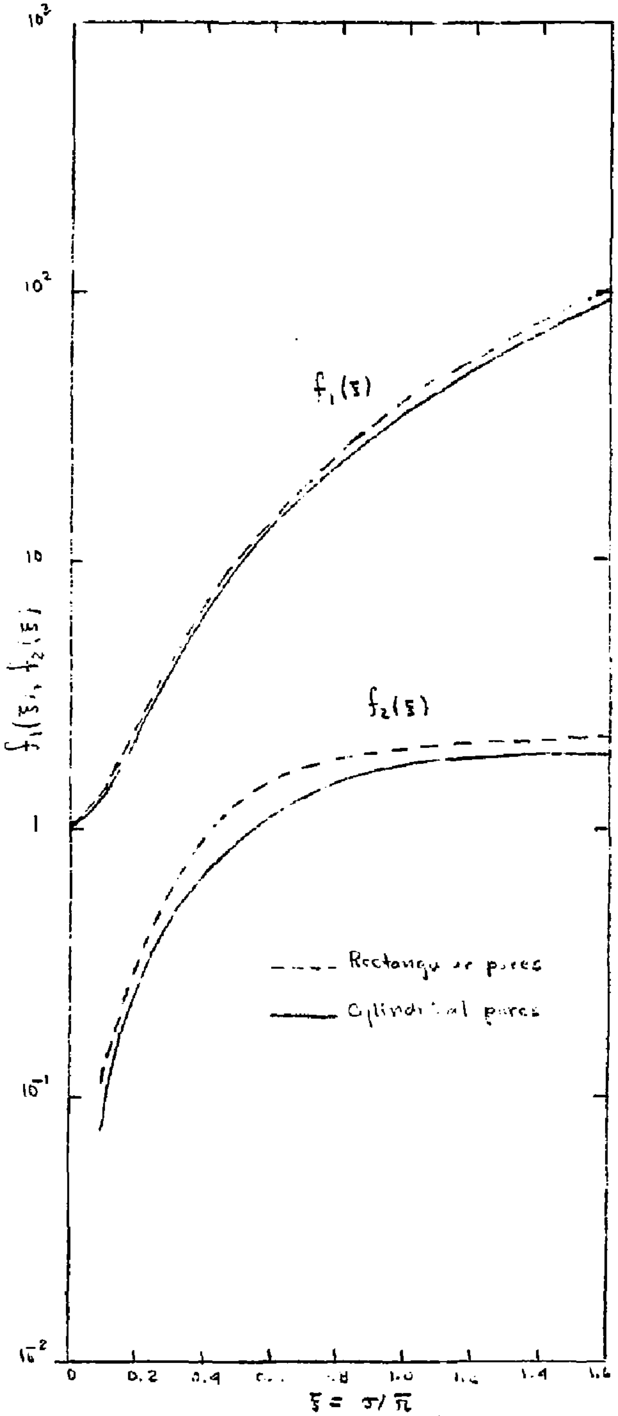

Figure 2
$f_1(\xi)$ and $f_2(\xi)$ for both rectangular and cylindrical pores.

JH T

$$D^* = \frac{\{D\}^*}{\mathcal{D}} = 1 + \frac{1}{48} Pe^2 f_1(\xi) + Pe^2 f_2(\xi)\theta, \qquad (44)$$

using the following dimensionless variables,

$$Z = z\,\mathcal{D}/\{v_z\}\,\bar{r}^2, \quad \theta = t\mathcal{D}/\bar{r}^2, \quad \{C\}^* = \{c\}^*/c_0, \quad Pe = \{v_z\}\,\bar{r}/\mathcal{D} \qquad (45)$$

Equation (43) may be solved readily using Fourier Transforms for the case of a sharp input pulse placed at $Z = 0$ at time $\theta = 0$,

$$\{C\}^* = \delta(Z) \quad \theta = 0, \qquad (46)$$

so that,

$$\{C\}^* = \frac{Pe}{\sqrt{4\pi W(\theta)}} \exp\left[-\frac{(Z-\theta)^2 Pe^2}{4\,W(\theta)}\right] \qquad (47)$$

with

$$W(\theta) = [\,1 + \frac{1}{48} Pe^2 f_1(\xi)\,]\theta + Pe^2 f_2(\xi)\frac{\theta^2}{2} \qquad (48)$$

The effect of the pore size distribution on the spread of the pulse at a given value of Z is illustrated in Figure 3. Note that as the spread of the pore size distribution increases, the spread of the pulse is greatly magnified. For large values of θ, the pulse width is dominated by the θ^2 term in Eq. (48), pointing out the increased effect of the convective separation term.

4. Turbulent Flow Case

For the case of fully-developed turbulent flow in a smooth cylindrical pore, the velocity is related to the friction factor by the equation [6],

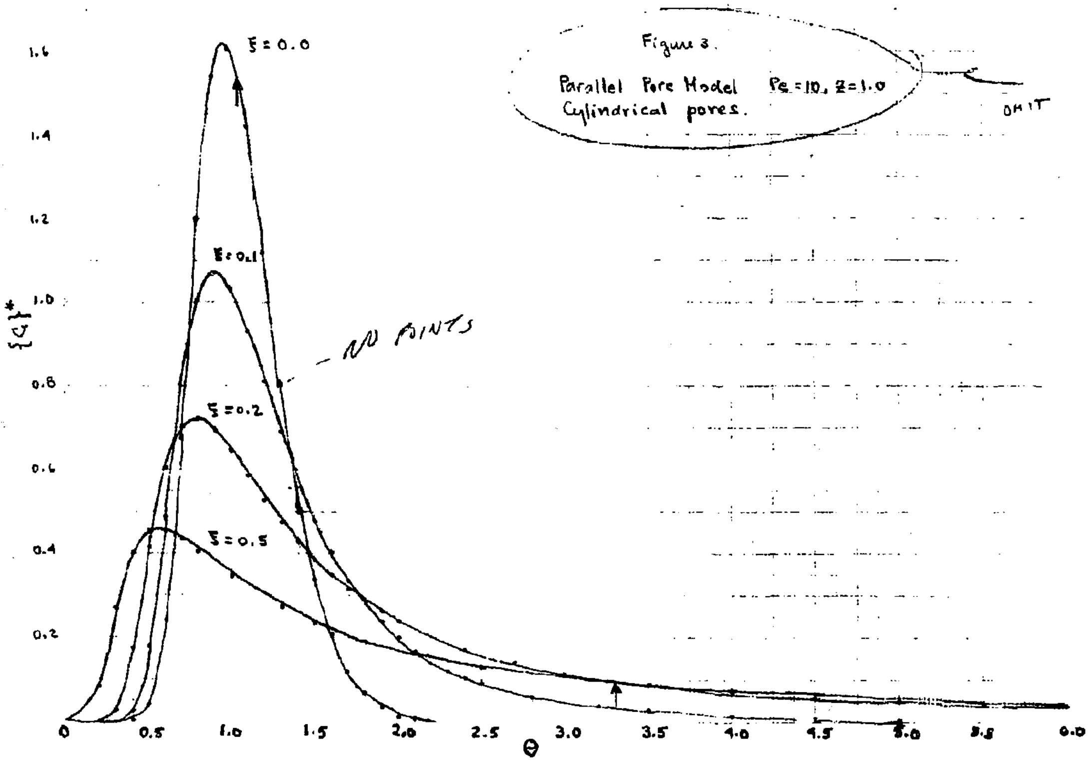

Figure 3.

Parallel Pore Model $Pe = 10$, $z = 1.0$
Cylindrical pores.

$$f = \frac{2r_i}{\frac{1}{2}\,\rho\langle v_z\rangle_i^2}\left(\frac{\Delta p}{L}\right) \qquad (49)$$

The friction factor under these conditions is well represented by the Blasius formula [6],

$$f = 0.316\ Re^{-1/4} \qquad (Re < 5\times10^5) \qquad (50)$$

where the Reynolds number is defined as,

$$Re = \langle v_z\rangle_i\ 2r_i/\nu \qquad (51)$$

with ν the kinematic viscosity. Combining Eqs. (49) and (51), we obtain an explicit relationship for $\langle v_z\rangle_i$,

$$\langle v_z\rangle_i = A\ r_i^{5/7} \qquad (52)$$

where,

$$A = \left[\frac{15.05}{\rho\nu^{1/4}}\left(\frac{\Delta p}{L}\right)\right]^{4/7} \qquad (53)$$

Using Eqs. (5) and (52), it is easy to show that for the case of cylindrical tubes,

$$\langle v_z\rangle_i = \{v_z\}\ \frac{r_i^{5/7}\sum_{i=1}^{N} r_i^2}{\sum_{i=1}^{N} r_i^{19/7}} \qquad (54)$$

This equation shows a much different relation between $\langle v_z\rangle_i$ and $\{v_z\}$ than the analogous Eq. (34) for laminar flow.

Taylor has used the universal velocity distribution for turbulent flow to calculate a dispersion coefficient for turbulent flow in a tube [10] in terms of the friction factor,

$$D_i = 10.1\ r_i \langle v_z\rangle_i \sqrt{\frac{1}{8} f} \qquad (55)$$

with f given by Eq. (50). Substituting Eq. (50) into (55) we obtain,

$$D_i = 1.8407\ \nu^{1/8}\ r_i^{\ 7/8} \langle v_z\rangle_i^{\ 7/8} \qquad (56)$$

so that upon substitution of Eq. (54),

$$D_i = 1.8407\ \nu^{1/8}\ \{v_z\}^{7/8}\ r_i^{\ 3/2} \left(\frac{\sum r_i^2}{\sum r_i^{19/7}} \right)^{7/8} \qquad (57)$$

Using Eqs. (26) and (54) we can calculate ω_i for turbulent flow,

$$\omega_i = \frac{r_i^{\ 19/7}}{\sum r_i^{\ 19/7}} \qquad (58)$$

In order to obtain the dispersion coefficient $\{D\}^*$ for the porous media in turbulent flow, we substitute Eqs. (54), (57) and (58) into Eq. (31),

$$\{D\}^* = 1.8407\ \nu^{1/8}\ \{v_z\}^{7/8}\ \frac{(\overline{r^{59/14}})(\overline{r^2})^{7/8}}{(\overline{r^{19/7}})^{15/8}} + \{v_z\}^2 t\ \frac{(\overline{r^2})}{(\overline{r^{19/7}})^2} \left[\frac{(\overline{r^2})(\overline{r^{29/7}})}{(\overline{r^{19/7}})} - \overline{r^{24/7}} \right] \qquad (59)$$

where for simplicity we have extended the definition of $\overline{r^n}$, Eq. (38), to non-integer values of n. Equation (59) should be compared to Eq. (39) for laminar flow. There are several obvious differences, but primarily we can point out the difference in the velocity dependence, the dependence on the pore size distribution, and the magnitudes of the coefficients in the equations. In the section that follows, we try to determine how the velocity dependencies of Eqs. (40) and (59) compare to the experimental results that have been obtained for dispersion coefficients in packed beds.

5. *Comparison to Experimental Data*

In a real porous media, the pores are not completely segregated as is the case in the model adopted here. This would tend to diminish the role of the contribution to {D}* from the convective terms that gave rise to the time-dependent term in Eq. (31). At best, the characteristic time for this separation to occ· ·ill be of the order of the pore length divided by the average velocity,

$$t_c = \ell/\{v_z\} \tag{60}$$

If the pore length is of the order of the pore radius, then Eq. (60) may be made dimensionless,

$$\theta_c = t_c \mathcal{D}/\bar{r}^2 = \mathcal{D}/\bar{r}\,\{v_z\} = Pe^{-1} \tag{61}$$

Substituting this value for the dimensionless time into Eq. (44), we obtain an expression for the dimensionless dispersion coefficient,

$$D^* = 1 + \frac{1}{48} Pe^2 f_1(\xi) + Pe\, f_2(\xi) \qquad (62)$$

From the curves shown in Figure 2, we have reason to suspect that the ratio f_2/f_1 for reasonably narrow size distributions $(0.1 < \xi < 0.5)$ is of the order of 10^{-1} so that we may write Eq. (62) as,

$$D^* = 1 + \left[\frac{Pe^2}{48} + 0.10\, Pe \right] f_1(\xi) \qquad (63)$$

The parameter f_1 may be treated as an adjustable parameter to fit data of D^* versus Pe in porous media. Bear [11] has summarized measured values of D^* from many investigators, and some representative results are given in Figure 4. These results are in terms of the particle Peclet number, defined as

$$Pe_p = \frac{\varepsilon \{v_z\}\, \bar{d}_p}{\mathcal{D}} \quad , \qquad (64)$$

where ε is the bed void fraction, and $\bar{d}_p$ is the average particle diameter. The points in this figure illustrate the trend and scatter in the more than 150 points in his comprehensive plot. There is data available through the entire range of Pe_p, not just at the isolated points shown in Figure 4 of this paper.

If we associate $\bar{r}$, the average pore radius in the parallel pore model, with the hydraulic radius for the packed bed [12], we can relate $\bar{r}$ to $\bar{d}_p$ for spherical particles,

$$\bar{r} \simeq \frac{\varepsilon}{1-\varepsilon} \frac{\bar{d}_p}{6} \qquad (65)$$

As a result, Pe and Pe_p are related by the equation,

$$Pe = Pe_p/6(1-\varepsilon). \qquad (66)$$

A good estimate of ε for packed beds is $\varepsilon = 0.40$, so that Eq. (66) yields $Pe = 0.278\ Pe_p$. Figure 4 shows Eq. (63) with this estimate for Pe in terms of Pe_p for the special case of $f_1(\xi) = 20.52$. The Pe_p dependence of the data matches very well the dependence predicted by Eq. (63) for all $Pe_p < 10^2$. For $Pe \geq 10^2$, this equation greatly overestimates the value of D^*. The theory lies above the data for $Pe_p \to 0$ since it does not take into account the effect of the void fraction of the bed or tortuosity of the pores. According to Figure 2, a value of $f_1(\xi) = 20$ corresponds to a $\xi = \sigma/\bar{r} = 0.75$, which is less than one, as might be expected.

If we substitute the estimate for the characteristic time t_c from Eq. (60) into the equation for $\{D\}^*$ for turbulent flow, Eq. (59), and make it dimensionless, we obtain,

$$D^* = 1.8407\ S_c^{1/8}\ Pe^{7/8}\ g_1(\xi) + Pe\ g_2(\xi) \qquad (67)$$

where $g_1(\xi)$ and $g_2(\xi)$ are the analogs of the functions $f_1(\xi)$ and $f_2(\cdot)$ for turbulent flow. Note that Eq. (60) predicts a slight Schmidt number dependence for D^*. This dependence is so weak that it might easily be masked by errors in experimental measurements of D^*. Using the value of $\xi = 0.75$ used to fit the data in the laminar flow region and calculating $g_1(\xi)$ and $g_2(\xi)$ from the moment expressions, we obtain

$g_1 = 1.945$ and $g_2 = 0.081$. In Figure 4 we plot Eq. (67) with these values of g_1 and g_2 using the relationship $Pe = 0.278\ Pe_p$. The slope of the curve of D^* as a function of Pe_p matches very well with the slope of the experimental data, but the predicted D^* values are too small by a factor of 4.20 when $Sc = 1.0$. With $Sc = 10^3$, the agreement is better.

It could be argued that the agreement between the results of this admittedly heuristic analysis and experimental data is fortuitous. However, it would not be unreasonable to suspect that the elementary model adopted here has some of the elements present in real flows in packed beds. The variation in slope of the D^* versus Pe_p curve is explained by our model as being caused by a continuous transition from fully laminar flow to a flow having turbulent characteristics. The transition from one type of flow to the other could occur anywhere in the Pe_p range $10 < Pe_p < 10^2$, possibly accounting for the large degree of scatter in the data near $Pe_p = 50$.

Eq. (40), with the estimate for the characteristic time t_c substituted in for t, takes the form.

$$\{D\}^* = \mathcal{D} + \frac{\{v_z\}^2\ \bar{r}^2}{48\ \mathcal{D}}\ f_1(\xi) + \{v_z\}\ \ell\ f_2(\xi) \qquad (68)$$

According to the relationship between $\bar{r}$ and $\bar{d}_p$, Eq. (65), as the mean particle diameter increases, the mean pore radius will increase, and as the spread of the particle size distribution increases, so will the spread of the pore size distribution. Eq. (68) can be used to make some predictions regarding the effect of the mean particle size and particle size distribution.

First, one can predict that for small particles ($\bar{r}$ small), the dependence of $\{D\}^*$ on $\{v_z\}$ should be linear, while for large particles ($\bar{r}$ large), the dependence on $\{v_z\}$ should be second order. Furthermore, Eq. (69) predicts, as we have indicated earlier, that $\{D\}^*$ should increase as the spread of the particle size distribution increases (ξ increases).

Table 1 summarizes the results of some measurements made by Niemann [13], of the dispersion coefficient for liquid in packed beds for particle sizes ranging in diameter from 0.03 to 0.15 mm for the small particles and from 0.15 to 0.75 mm for the large particles. Values of $\{v_z\}$ were very small, in the range $0.4 < \{v_z\} < 1.5$ cm/min. For the small particle sizes the power on the velocity was of the order 1.0 as predicted. For the larger particles the power on $\{v_z\}$ was between 1. and 2.0. In all cases, the wider the spread of the particle size distribution, the larger the dispersion coefficient. The bed void fraction remained essentially constant for all these experiments. These results present additional support for the applicability of this simple dispersion model to dispersion in packed beds.

Figure 4

D^* dependence on Pe_p as reported by Bear [11], compare to Eqs. (67) and (68).

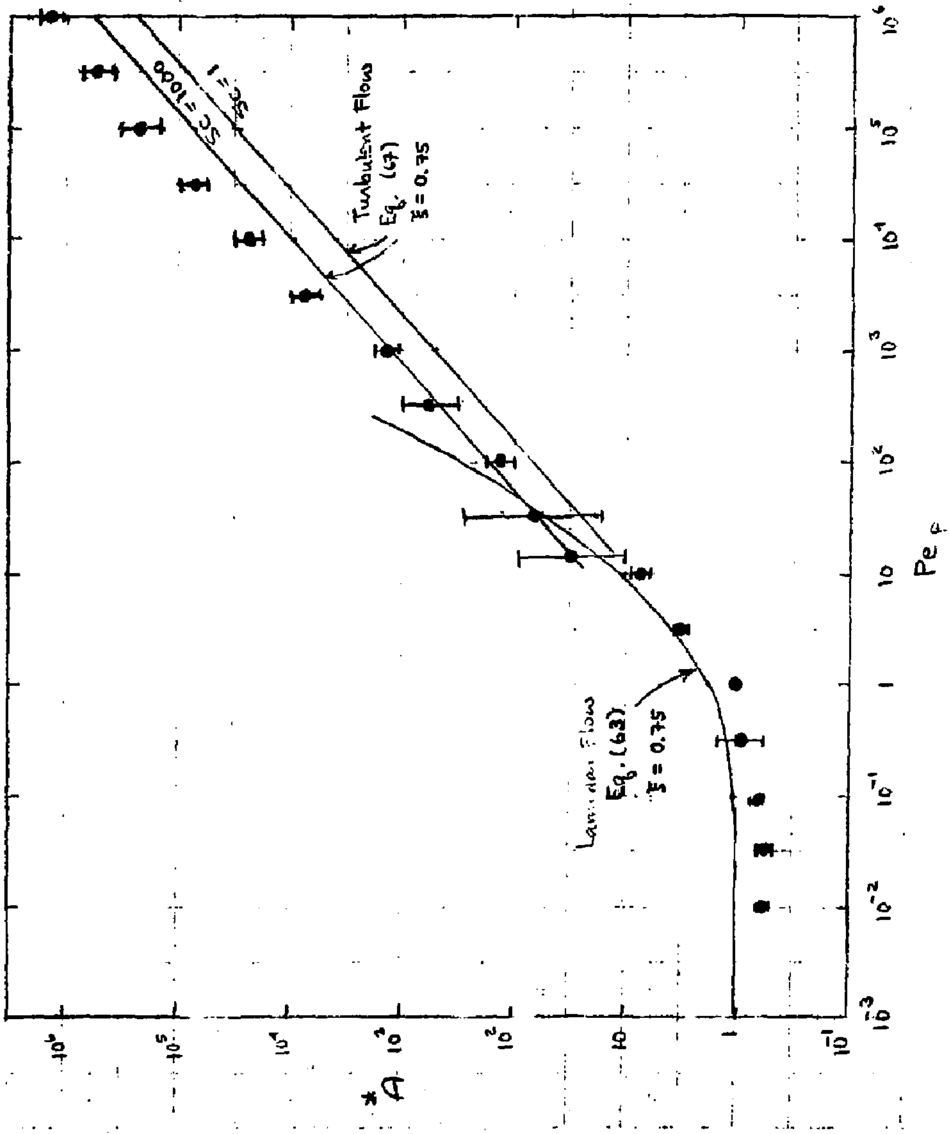

$$\{D\}^* \; (cm^2/min) = (a \times 10^{-3}) \; \{v_z\}^m$$

$$(\; \{v_z\} \;\; \text{in cm/min})$$

Experiment	Description	a	m
1	Small beads, small spread of particle size distribution	0.51	0.96
2	medium spread	0.71	1.04
3	large spread	1.0	0.97
4	Large beads, small spread	0.39	1.40
5	medium spread	0.68	1.60
6	large spread	0.78	1.51

TABLE 1

Results of Niemann's [13] experiments for dispersion coefficients for different particle size distributions

APPENDIX

Proof that $m_{ob} = m_o$

In the context of the Taylor-Aris theory, the concentration at any point in a cylindrical tube is related to the area-averaged concentration $\langle c \rangle_i$ by the equation,

$$c_i = \langle c \rangle_i + F(r) \frac{\partial \langle c \rangle_i}{\partial z} \qquad \text{(A.1)}$$

where $F(r)$ is a function of radial position. The bulk-averaged concentration c_{bi} is defined by,

$$\langle v_z \rangle_i \, c_{bi} = \langle v_z(r) c_i(r) \rangle \qquad \text{(A.2)}$$

where the brackets represent the area integral in cylindrical coordinates. Substituting (A.1) into (A.2) we find,

$$\langle v_z \rangle_i \, c_{bi} = \langle v_z \rangle_i \langle c \rangle_i + \langle v_z F \rangle \frac{\partial \langle c \rangle_i}{\partial z} \qquad \text{(A.3)}$$

Taking the zeroth moment of both sides of A.3 with respect to z, one can show immediately that,

$$m_{obi} = m_{oi} \qquad \text{(A.4)}$$

since for a pulsed system $\langle c \rangle_i = 0$ at $z = \pm \infty$. Since Eq. (A.4) holds in each pore, Eq. (13) holds for the porous media as a whole.

Higher moments of a Gaussian distribution

For a given distribution of the type,

$$p(r)\,dr = \frac{1}{\sigma\sqrt{2\pi}} \exp\left[\frac{-(r-\bar{r})^2}{2\sigma^2}\right] \tag{A.5}$$

the nth moment of the distribution,

$$\overline{r^n} = \int_{-\infty}^{\infty} r^n\, p(r)\, dr \tag{A.6}$$

may be calculated using the generating function,

$$\phi(u) = \exp[i\bar{r}u - \sigma^2 t^2/2] \tag{A.6}$$

by the formula,

$$i^n\, \overline{r^n} = \left.\frac{d^n\phi(u)}{du^n}\right|_{u=0} \tag{A.7}$$

carrying out the indicated operations, we calculated $\overline{r^2}$ through $\overline{r^{10}}$ inclusive,

$$\begin{aligned}
\overline{r^2} &= (1 + \xi^2)\,\bar{r}^2 \\
\overline{r^3} &= (1 + 3\xi^2)\,\bar{r}^3 \\
\overline{r^4} &= (1 + 6\xi^2 + 3\xi^4)\,\bar{r}^4 \\
\overline{r^5} &= (1 + 10\xi^2 + 15\xi^4)\,\bar{r}^5 \\
\overline{r^6} &= (1 + 15\xi^2 + 45\xi^4 + 15\xi^6)\,\bar{r}^6 \\
\overline{r^7} &= (1 + 21\xi^2 + 105\xi^4 + 105\xi^6)\,\bar{r}^7 \\
\overline{r^8} &= (1 + 28\xi^2 + 210\xi^4 + 420\xi^6 + 105\xi^8)\,\bar{r}^8
\end{aligned} \tag{A.8}$$

$$\overline{r^9} = (1 + 36\xi^2 + 378\xi^4 + 1260\xi^6 + 945\xi^8)\,\bar{r}^9$$

$$\overline{r^{10}} = (1 + 45\xi^2 + 630\xi^4 + 3150\xi^6 + 4725\xi^8 + 945\xi^{10})\,\bar{r}^{10}$$

where $\xi = \sigma/\bar{r}$. The functions $f_1(\xi)$ and $f_2(\xi)$ are obtained by substituting the expressions (A.8) into the terms containing the $\overline{r^n}$ in Eq. (39), namely,

$$\frac{\overline{r^{10}}\,(\overline{r^2})^2}{(\overline{r^4})^3} = f_1(\xi)\,\bar{r}^2 \qquad \text{(A.9)}$$

$$\frac{\overline{r^2}}{(\overline{r^4})^2}\left[\frac{\overline{r^2}\;\overline{r^8}}{\overline{r^4}} - \overline{r^6}\right] = f_2(\xi) \qquad \text{(A.10)}$$

ACKNOWLEDGEMENT

The author wishes to thank Professor S. Whitaker for helpful comments and suggestions, and Dr. R. Lyczkowski for agreeable discussions.

NOTATION

A	constant in Eq. (52)
A_i	area of pore i
A_p	total area of pores
c_{bi}	bulk-averaged concentration in pore i
c_i	point concentration in pore i
c_0	characteristic concentration
$\langle c\rangle_i$	area-averaged concentration in pore i
$\{c\}$	area-averaged concentration in porous media

$\{c\}_b$	bulk-averaged concentration
$\{c\}_D$	concentration defined by Eq. (8)
$\{c\}^*$	solution to dispersion equation
$\{C\}^*$	dimensionless $\{c\}^*$
$\bar{d}_p$	mean particle diameter
D_i	dispersion coefficient in pore i
$\{D\}$	coefficient defined by Eq. (6)
$\{D\}^*$	dispersion coefficient in dispersion equation
D^*	dimensionless $\{D\}^*$
$\mathcal{D}$	molecular diffusivity
f	friction factor
$f_1(\xi)$, $f_2(\xi)$	functions of the ratio ξ for laminar flow
$F(r)$	function multiplying gradient of $\langle c\rangle_i$
$g_1(\xi)$, $g_2(\xi)$	functions of the ratio ξ for turbulent flow
ℓ_i	half gap width for rectangular pore
$\bar{\ell}$	average value of ℓ_i
ℓ	characteristic pore length
m_k	kth axial moment of $\{c\}$
m_{ki}	kth axial moment of $\langle c\rangle_i$
m_{kb}	kth moment of $\{c\}_b$
m_{obi}	zeroth moment of c_{bi}
m_{oD}	zeroth moment of $\{c\}_D$
$p(r)\,dr$	pore size distribution
Pe	Peclet number $\{v_z\}\,\bar{r}/\mathcal{D}$
Pe_p	particle Peclet number $\varepsilon\{v_z\}\,\bar{d}_p/\mathcal{D}$
r	radial position in a given pore
r_i	radius of pore i

$\bar{r}$	average pore radius
$\overline{r^n}$	nth moment of pore size distribution
Sc	Schmidt number, ν/D
t	time
$v_z(r)$	velocity profile in a given pore
$\langle v_z \rangle_i$	area-averaged fluid velocity in pore i
$\langle v_z \rangle$	area-averaged fluid velocity in porous media
$W(\theta)$	function defined by Eq. (48)
z	axial position
Z	dimensionless axial position

Greek Symbols

σ	standard deviation of pore size distribution
θ	dimensionless time
ζ	$\sigma/\bar{r}$
ω_i	fraction of the total amount of solute in pore i

REFERENCES

1. Greenkorn, R. A. and D. P. Kessler, in "Flow Through Porous Media", American Chemical Soc., Washington, D. C., 1970, p. 159.

2. Haring, R. E. and R. A. Greenkorn, AIChE Journal, 1970, 16, 477.

3. Saffman, P. G., J. Fluid Mech., 1959, 6, 321.

4. De Josselin De Jong, G., Trans. AM. Geophys. Union, 1956, p. 595.

5. Whitaker, S., AIChE Journal, 1967, 13, 420.

6. Whitaker, S., "Introduction to Fluid Mechanics", Prentice Hall, Englewood Cliffs, N. J., 1968.

7. Taylor, G. I., Proc. Roy. Soc. (London), 1953, A219, 186.

8. Aris, R., Proc. Roy. Soc. (London), 1956, A235, 67.

9. Abramowitz, M. and I. A. Stegun, "Handbook of Mathematical Functions", Dover Publications, N. Y., 1965, p. 928 ff.

10. Taylor, G. I., Proc. Roy. Soc. (London), 1954, A223, 446.

11. Bean, J., in "Flow Through Porous Media", R. de Wiest, Ed., Academic Press, New York, 1969, Ch. 4.

12. Bird, R. B., W. E. Stewart and E. N. Lightfoot, "Transport Phenomena", J. Wiley and Sons, Inc., New York, 1960, p. 199 ff.

13. Niemann, E. H., M. S. thesis, Purdue University, Lafayette, Ind., 1969.

List of Figures:

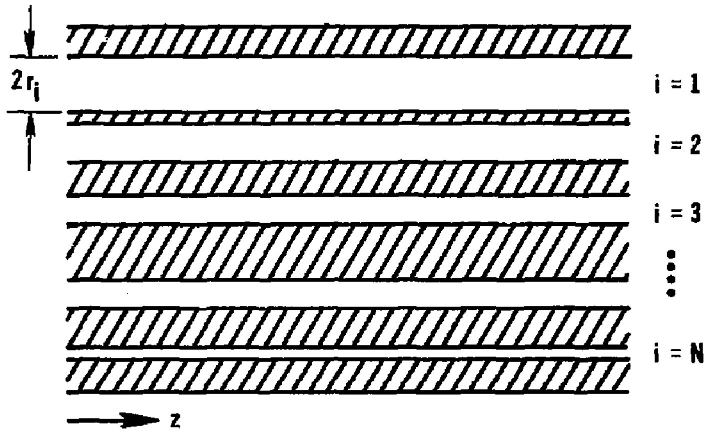

Figure 1:

The parallel pore model

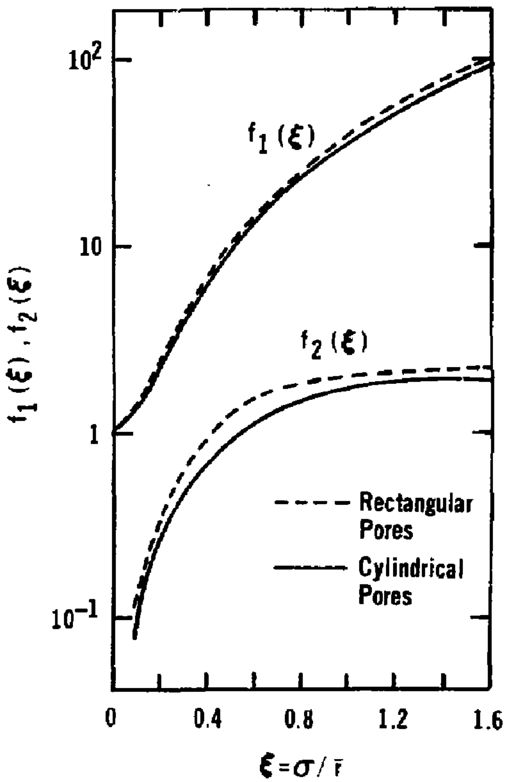

Figure 2:
Functions f_1 and f_2 for rectangular and cylindrical pores

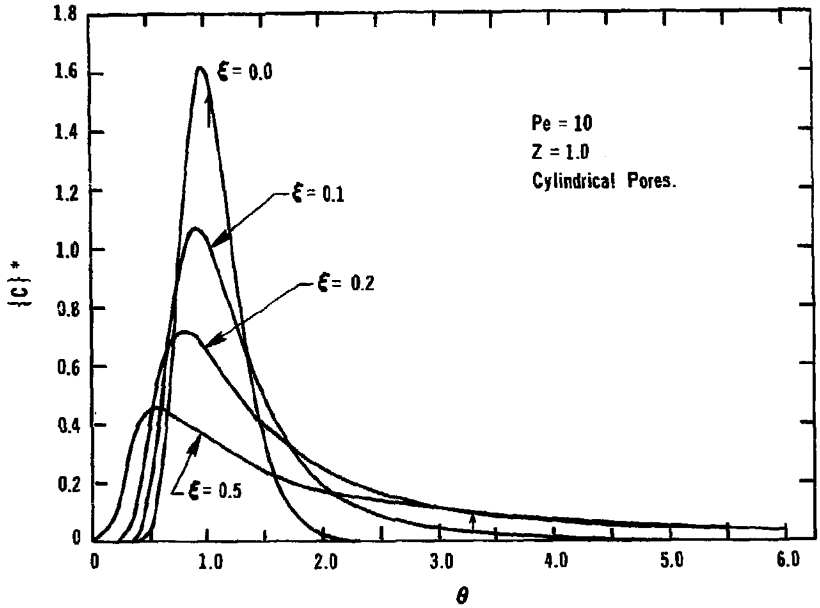

Figure 3:

Concentration as a function of time for $Z = 1.0$, $Pe = 10$, and cylindrical pores in laminar flow

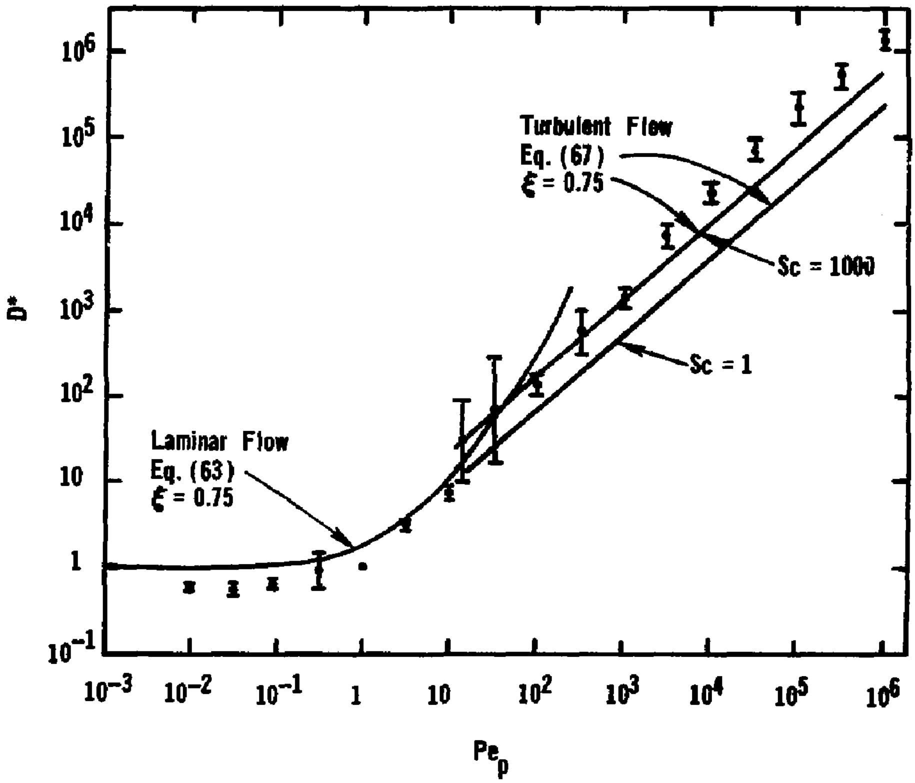

Figure 4:

D* dependence on Pe_p as reported by Bear [11], compared to laminar and turbulent flow equations with $\xi = 0.75$